RSC Advances

ROYAL SOCIETY OF CHEMISTRY

www.rsc.org/advances

Effect of ionic liquid-containing poly (ε-caprolactone) on dispersion and dielectric properties of polymer/carbon nanotubes composites

Ye Ren[a], Zheng Zhou[a], Guangzhong Yin[b], Guang-Xin Chen[a,*], Qifang Li[b,*]

a Key Laboratory of Carbon Fiber and Functional Polymers, Ministry of Education, Beijing University of Chemical Technology, Beijing 100029, P. R. China

b College of Material Science and Engineering, Beijing University of Chemical Technology, Beijing 100029, P. R. China

*Corresponding author: gxchen@mail.buct.edu.cn(G.-X. Chen). FAX: +86-10-64421693; qflee@mail.buct.edu.cn (Q. Li). FAX: +86-10-64433585

Abstract

Supramolecular chemistry is a reliable and effective field that encompasses the functionalization of carbon nanotubes (CNTs) through non-covalent interactions, such as π-π stacking and cation–π interactions. In this work, poly(ε-caprolactone) (PCL) containing an ionic liquid group was synthesized through ring-opening polymerization of ε-caprolactone by using hydroxylated ionic liquid derived from imidazole and 2-Bromoethanol. Ionic liquid-containing PCL exhibited affinity for the π-conjugated structure in CNTs. The fabricated PCL/CNTs composite showed improved CNTs dispersion because of the addition of ionic liquid-containing PCL as compatibilizer. The composite also demonstrated enhanced electronic and dielectric properties as a result of the excellent interfacial control by the compatibilizer, which could be due to the anchoring of PCL chains onto the CNTs surface via non-covalent (supramolecular) functionalization. This simple approach provides novel supramolecular tools for using renewable resources to prepare CNTs-based composites with high performance.

Keywords: Ionic Liquid; Carbon nanotube; Poly (ε-caprolactone).

1. Introduction

Carbon nanotubes (CNTs) are novel nanostructures with widespread applications in functional materials. With their unique properties, CNTs are used as supports for catalysis and as nanofillers for polymeric composites to develop electrochemical and energy storage devices. Increased interest on the unique structure of the multiple concentric cylinders of CNTs leads to technological and scientific advances in the development of CNTs-based nanostructured compounds [1-8]. CNTs exhibits promising applications in polymer nanocomposites, which are polymer matrix incorporated with nanoscale filler materials [9, 10]. Uniformly dispersed CNTs may amend the structure–property features of polymers to a great extent [11, 12].

CNTs tend to aggregate in organic solvents and aqueous dispersions because of their strong intermolecular π-π stacking interaction, which leads to bundle arrangement, a major limitation for processing of CNTs. In this regard, "grafting from" and "grafting onto" techniques are performed to disperse and improve interfacial adhesion within polymeric matrices [13, 14]. However, these techniques involve creating a covalent bond between polymer chains and substrate surface, thereby producing structural defects on the conjugated CNTs surface and adversely affecting the electrical and mechanical properties of the composites [15]. A potential compound used to address this limitation is imidazolium ionic liquids (ILs), which exhibit affinity for the CNTs surface [16-18]. Imidazolium rings can be adsorbed onto the conjugated π structure because of cation-π and π-π interactions, resulting in disentanglement of CNTs bundle [19-22]. This strategy is a simple and cost-effective technique for preserving the electronic structure of CNTs [23, 24] and their intrinsic properties [25].

Poly(ε-caprolactone) (PCL) is a biodegradable and biocompatible synthesis material with immense potential for applications in bionanoscience and technology [26]. The use of PCL for nerve regeneration or in spinal cord repair requires the polymer to be highly electrically conductive, which can be achieved through CNTs addition [27]. The addition of CNTs also provides numerous potential applications, such as conducting substrates for EMI shielding and electronic devices [28].

Specific interactions between CNTs and imidazolium ions provides novel application prospects because imidazolium ILs can be easily functionalized by attaching polymeric chains [29]. In this regard, the incorporation of an imidazolium group on the polymeric backbone is an

efficient strategy for improving CNTs interaction and dispersion within polymer matrices [30, 31]. Hence, a new and straightforward approach must be developed to disperse CNTs and prepare PCL/CNT composites.

In this work, a PCL block copolymer consisting of IL segment (ImPCL) was synthesized through ring-opening polymerization (ROP) and used as interfacial controller (compatibilizer) between CNTs and PCL. The imidazolium ring segment can interact with CNTs via π-π stacking interaction, whereas the PCL block segment was compatible with the PCL matrix. This study aims to demonstrate the ability of PCL chains with the imidazolium ring segment in improving CNTs dispersion within the PCL matrix. Electrical, dielectric, and morphological measurements were also conducted to assess CNTs dispersion in the polymer matrix prepared with and without the dispersing agent and confirm the establishment of supramolecular cation–π interaction between ImPCL and CNTs.

2. Experimental

2.1. Materials

Pristine multi-walled CNTs (MWCNTs), with diameter ranging from 40 nm to 60 nm and average length of less than 2 μm, were purchased from Carbon Nanotechnologies, Inc., China. ε-Caprolactone (ε-CL, Alfa Aesar) was purified through toluene azeotropic distillation (50 g/100 mL) using the Dean–Stark apparatus for 2 d. PCL (Mn = 47000 g/mol, Alfa Aesar) was dried in a vacuum oven for 24 h at 50 °C. N,N-Dimethylformamide was purified through distillation over CaH_2. 2-Bromoethanol (99%), imidazole (> 99%), and stannous octoate ($Sn(oct)_2$) (99%) were purchased from Alfa Aesar and used as received. Other solvents, such as ethanol and sodium, were obtained from Beijing Chemical Works.

2.2. Synthesis of ImPCL

Imidazolium-containing segmented PCL was synthesized through ROP of ε-CL by using 1,3-di(2-hydroxyethyl) imidazolium bromine (HHIM) as macro initiator and stannous octoate as catalyst [32]. Briefly, 300 mg of HHIM [33] prepared in our lab, 10.0 g of ε-CL, and 20 mL of DMF were weighed into an eggplant-type reaction flask. The flask was immersed in an oil bath at 100 °C under magnetic stirring for 24 h. After the reaction, the product was precipitated into ether

or methanol (500 mL). After filtration and drying in a vacuum oven at 60 °C for 24 h, a white powder was obtained.

2.3. Preparation of PCL/ImPCL/CNT composites

Pristine MWCNTs and ImPCL were mixed in dichloromethane and subjected to mild ultrasonic treatment to obtain a black homogeneous dispersion. PCL solution was prepared by dissolving PCL in dichloromethane. The PCL solution was mixed with the MWCNT dispersion to fabricate a composite membrane. The mixture was casted onto a PTFE plate and then dried at room temperature. The final product, labeled as PCL/ImPCL/CNTs (Table 1), was dried in a vacuum oven at 60 °C to remove the residual solvent.

Table 1. Sample composition with and without ImPCL.

	PCL (g)	ImPCL (g)	CNTs (g)
PCL/10%ImPCL/0%CNTs	4.5	0.5	0
PCL/10%ImPCL/0.5%CNTs	4.475	0.5	0.025
PCL/10%ImPCL/1%CNTs	4.45	0.5	0.05
PCL/10%ImPCL/3%CNTs	4.35	0.5	0.15
PCL/10%ImPCL/4%CNTs	4.30	0.5	0.20
PCL/10%ImPCL/5%CNTs	4.25	0.5	0.25
PCL/10%ImPCL/6%CNTs	4.2	0.5	0.30
PCL/0%CNTs	5.00	0	0
PCL/0.5%CNTs	4.975	0	0.025
PCL/1%CNTs	4.95	0	0.05
PCL/3%CNTs	4.85	0	0.15
PCL/4%CNTs	4.8	0	0.20
PCL/5%CNTs	4.75	0	0.25

PCL/6%CNTs	4.7	0	0.30

2.4. Characterization

^{1}H NMR spectra were recorded at 400MHz in the AV400 (BRUKER) at 25^{o}C with deuterium solvents and TMS as an internal reference. Fourier transform infrared (FTIR) spectra were recorded with Bruker Tensor-27 Fourier transform infrared spectrometer by using the KBr disk method. Gel permeation chromategraphy (GPC) was performed on the system (Water 1515, Isocratic HPLC Pump and Water 2414 Refractive index Detector) to obtain the molecular weight and poly dispersity index (PDI) of polymers at room temperature. THF was used as mobile phase with a flow rate of 1.0mL/min with column temperature at 31^{o}C, and monodisperse polystyrene standard samples were used for calibration. Differential scanning calorimetry **(**DSC) was performed using a DSC-200PC (NETZSCH). Raman spectroscopy (inVia model, Renishaw plc) at 514 nm with a 1.5 cm^{-1} resolution was used to confirm the CNTs structure. Field Emission Scanning Electron Microscope (FE-SEM) was performed with HITACHI S-4700 (FEI) microscope at an accelerating voltage of 20 kV. Dielectric properties and AC conductivity were measured by Agilent 4294A with 16451B fixture (40Hz~10MHz) at a room temperature. Uniaxial tensile tests were carried out at 25 ^{o}C with a crosshead speed of 50 mm·min^{-1}. Samples measuring 20 mm×4 mm×0.5 mm were cut from films obtained using a fresh razor blade. The modulus of each sample was determined by linearly fitting the elastic portion of the stress-strain curve before the yielding point.

3. Results and discussion

3.1. Characterization of HHIM and ImPCL

ROP is an efficient method used to prepare PCL and poly(lactic acid). Initiated by alcohol or water and in the presence of $Sn(OCT)_2$ as catalyst, a macromolecule fitted with a terminal hydroxyl constantly propagates for chain-extension reaction and eventually forms a well-defined macromolecule containing the initiator segment. In our research, as a compatibilizer between PCL and CNTs, the well-defined polymer consisting of PCL and ILs was synthesized via ROP initiated by ILs containing two hydroxyl groups. Figure 1 shows the ^{1}H NMR spectrum of polymerization

product and characteristic peaks were tagged in it. It's worth noting that in the low-field of spectrum, two signals, at 9.16 ppm and 7.76 ppm, belonging to aromatic rings derived from imidazole are observed. The characterization and analysis for ImPCL prove that polymerization was initiated by the designed initiator. The molecular weight of ImPCL determined by GPC in THF was 11946 and the distribution was 1.38.

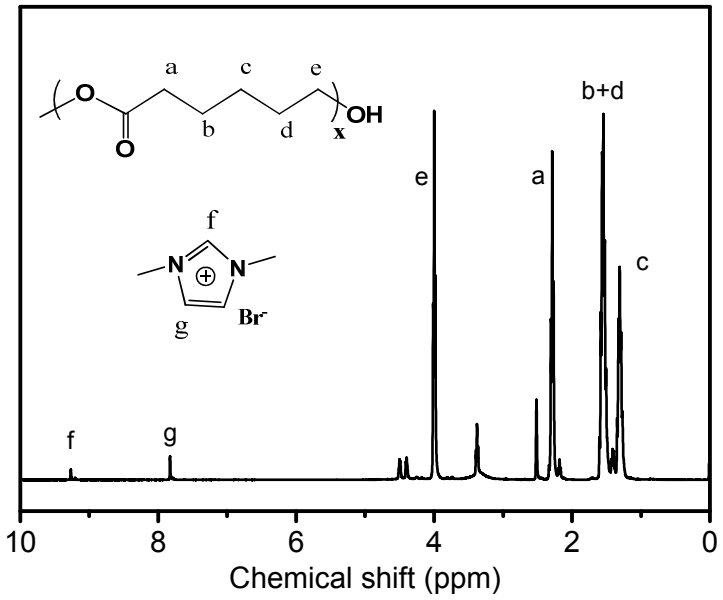

Figure 1. ^{1}H NMR of ImPCL in DMSO.

3.2. ImPCL/CNTs hybrid

In order to elucidate the performance of CNTs dispersion, we performed a visual dispersion test by using a simple procedure. ImPCL and MWCNT solutions were separately prepared and then mixed. The mixture was sonicated for 60 min to obtain ImPCL-coated CNTs (ImPCL/CNTs), whose ILs segments could wrap on MWCNTs through π-π stacking interaction. Centrifugation and filtration were repeated several times to obtain the purified ImPCL/CNTs hybrid. The hybrid shows excellent dispersion stability (Figure 2) in dichloromethane and other organic solvents, such as toluene, chloroform, and THF after standing 48 hours.

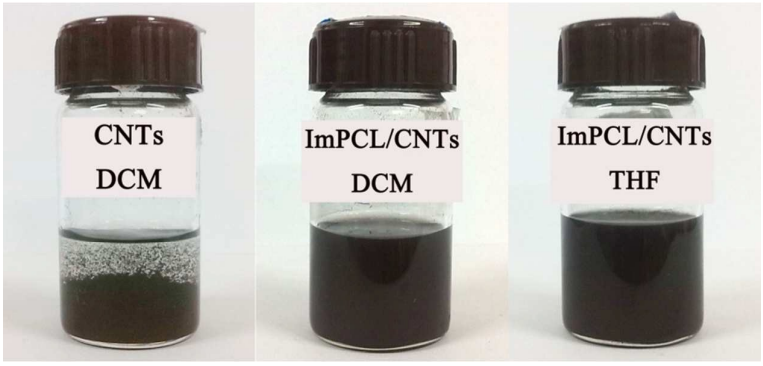

Figure 2. CNTs dispersion test with and without ImPCL in organic solvent

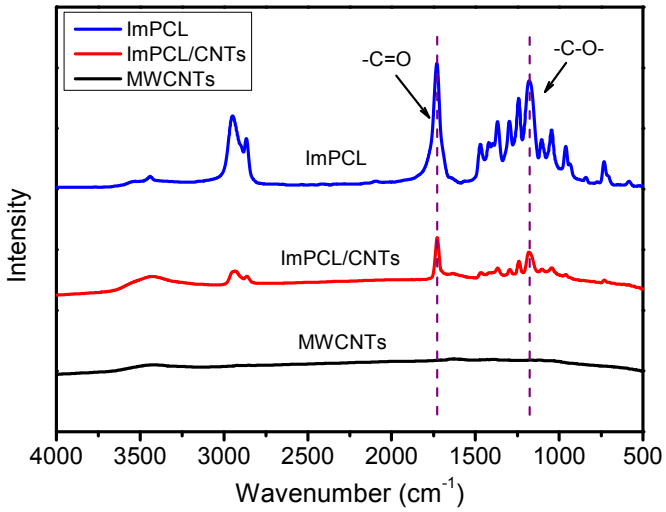

Figure 3. FTIR spectra of MWCNTs, ImPCL, and ImPCL/CNTs.

The FTIR spectra of MWCNTs, ImPCL, and ImPCL/CNTs are shown in Figure 3. In ImPCL, the peaks at 2947 and 2866 cm^{-1} are assigned to the asymmetric and symmetric stretching vibrations of C-H bonds, respectively. The peaks at 1730 and 1174 cm^{-1} correspond to –C=O and C-O-C of the ester group. The absorption peaks of ImPCL/CNTs are identical with those of ImPCL, and the strong carbonyl stretching band at 1730 cm^{-1} indicates that the PCL molecules are attached to the surface of MWCNTs. By contrast, the characteristic absorption signal for MWCNTs is very weak, and the strong carbonyl stretching band is not present in the spectrum of the pristine MWCNTs. These results suggest that the polymer chain is successfully wrapped on the surface of MWCNTs with imidazole segments.

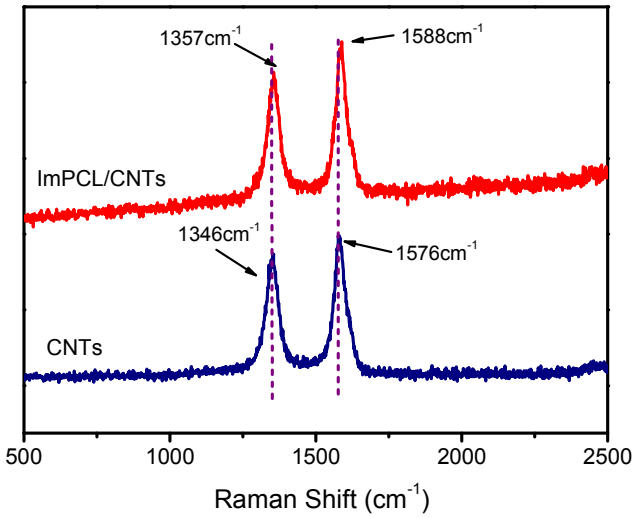

Figure 4. Raman spectra of CNTs and ImPCL/CNTs.

Raman spectroscopy is a direct and nondestructive technique used to characterize the structure and quality of carbon materials, particularly to determine defects, ordered, and disordered structures. The Raman spectra of MWCNTs exhibit two remarkable peaks at around 1350 and 1580 cm^{-1}, which correspond to the well-defined D and G bands, respectively. The G band related to the E_{2g} vibration mode of sp2 carbon domains can be used to explain the degree of graphitization, whereas the D band is associated with the structural defects and partially disordered structures of the sp3 domains [34, 35]. Structural alterations can induce changes in the Raman spectra of the samples; as such, the peak shape of D and G bands changes upon structural alterations during modification. For comparison, the spectra of pristine MWCNTs and ImPCL/CNTs were determined. Figure 4 shows the two peaks in both samples. The peak shape in ImPCL/CNTs does not significantly change compared with that in MWCNTs. More interestingly, the D band for CNTs (1346 cm^{-1}) shift to higher value (1357 cm^{-1}) upon addition of ImPCL and the G band shift from 1576 cm^{-1} to 1588 cm^{-1}. In addition, the ID/IG value of ImPCL/CNTs is similar to that of the pristine MWCNTs (ID/IG = 0.9), which indicating that the graphitization degree of the resultant hybrids are analogous to that of the pristine MWCNTs [15]. These findings demonstrate that the structure of CNTs in the hybrid remains unchanged, and the extended π-networks of the CNTs were not disrupted during coating.

3.3. PCL/ImPCL/CNT composites

CNTs distribution within the polymer matrix was examined via SEM. The SEM images (Figure 5) show the cross-sections of the composites prepared by fracturing in liquid nitrogen to produce an intact fractured surface. The broken ends of the CNTs pulled out from the fracture surface reveal the distribution of nanofillers within the polymer matrix. From Figure 5 (a) and (c) we can see, in the absence of compatilizer, large number of CNTs bundle together to form big agglomerations (areas marked in red), but in the other areas only few CNTs can be observed. For the PCL/ImPCL/CNTs composites (Figure 5 (b) and (d)), individual MWCNTs are visible in the matrix and no agglomerations are found throughout the observation field. These results indicate that ImPCL significantly exfoliate the CNTs bundles and improve the CNTs dispersion within the PCL matrix.

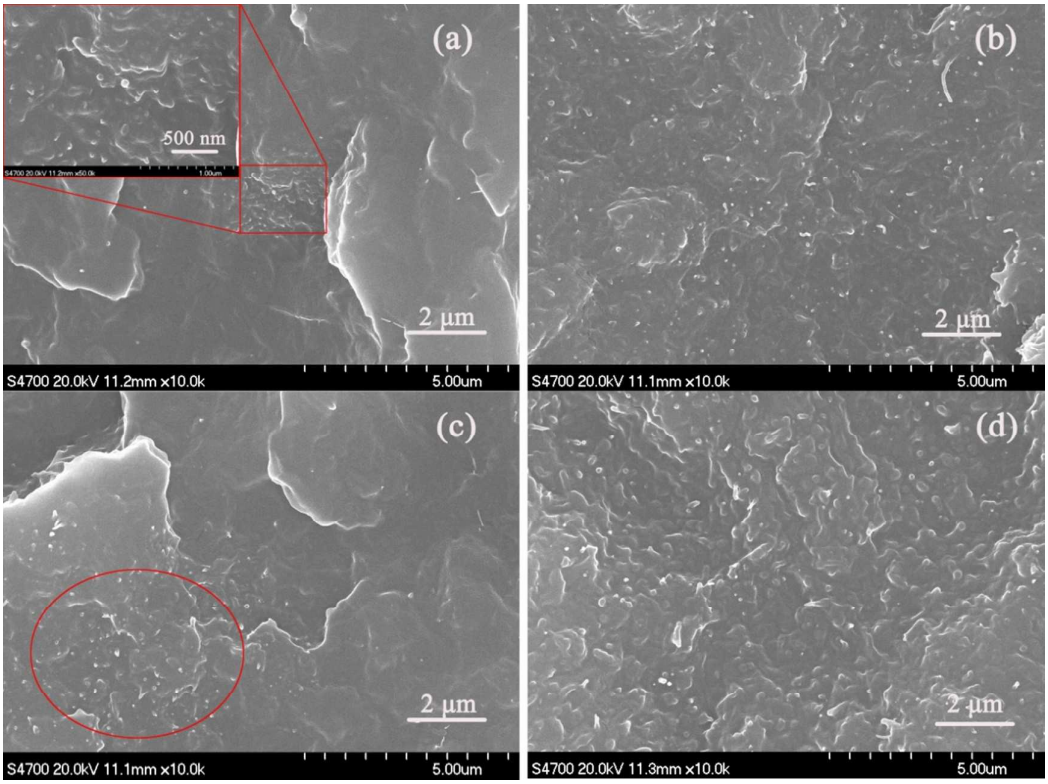

Figure 5. Cross-sectional SEM images of (a) PCL/3%CNTs, (b) PCL/10%ImPCL/3%CNTs, (c) PCL/5%CNTs, and (d) PCL/10%ImPCL/5%CNTs.

Figure 6 shows the DSC curves of neat PCL, PCL/ImPCL/CNTs (0.5–6 wt.% CNTs), and PCL/CNTs (0.5–6 wt.% CNTs), which are obtained after the second run under N_2 at 10 °C/min. The T_m of the neat PCL appears at 52.7 °C, which gradually increases to 55.7 °C in

PCL/ImPCL/CNTs with increasing CNTs content. The T_m of PCL/CNTs also increases to 55.5 °C, which is substantially lower than the corresponding PCL/ImPCL/CNTs with 6 wt.% CNTs. These results indicate that the PCL chains derive from ImPCL are homogeneously mixed with the PCL matrix, and both ImPCL and MWCNTs influence the crystalline structure of PCL. Interestingly, in PCL/10%ImPCL/0.5%CNTs, PCL/10%ImPCL/1%CNTs, and PCL/10%ImPCL/3%CNTs samples, small shoulder peaks appear before the melting peak. However, this phenomenon is not observed in PCL/CNTs samples and PCL/ImPCL/CNTs composites with high CNTs loadings. Mixed with PCL matrix, ImPCL affects the crystallinity and crystal wafer thickness of PCL, thereby forming some imperfect crystals during crystallization. These crystals may melt at lower temperatures compared with the perfect crystals. Moreover, the number of the interface in the composites increases with increasing filler content. Thus, the effect of ImPCL on the PCL matrix gradually decreases and eventually disappears. This phenomenon could be due to the existence of high amounts of ImPCL in the phase interface caused by interaction with CNTs.

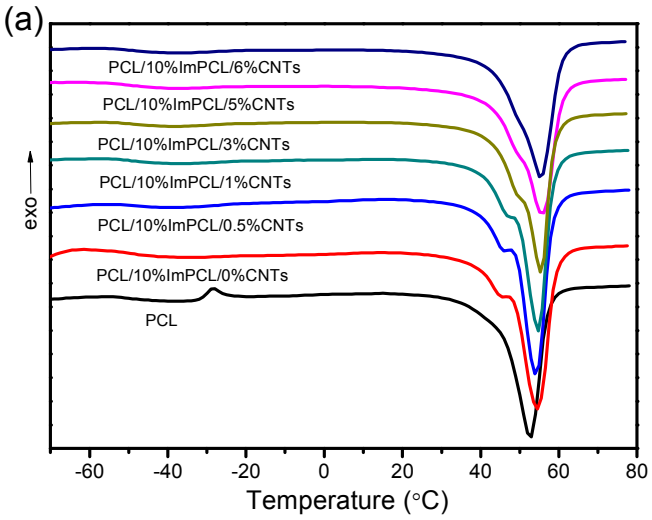

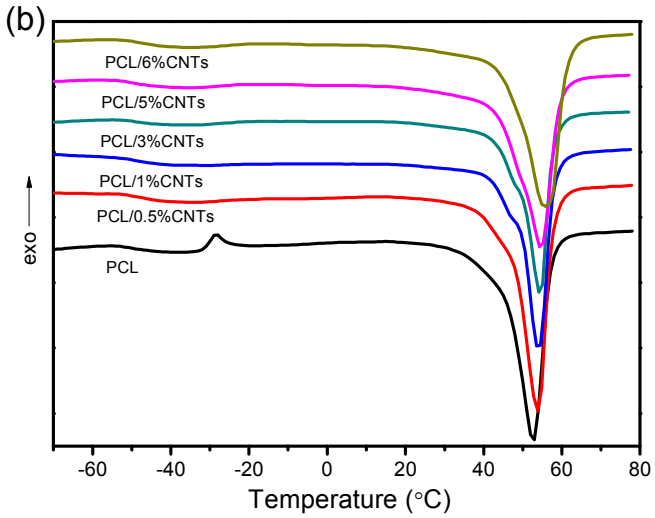

Figure 6. DSC thermograms of (a) PCL/ImPCL/CNTs and (b) PCL/CNT series.

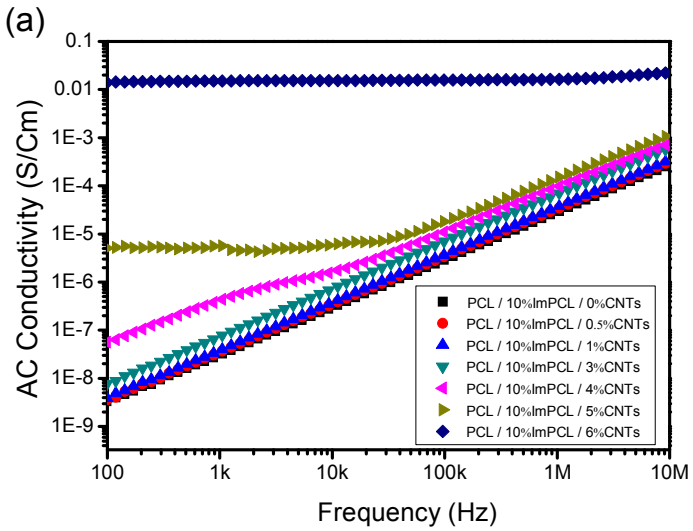

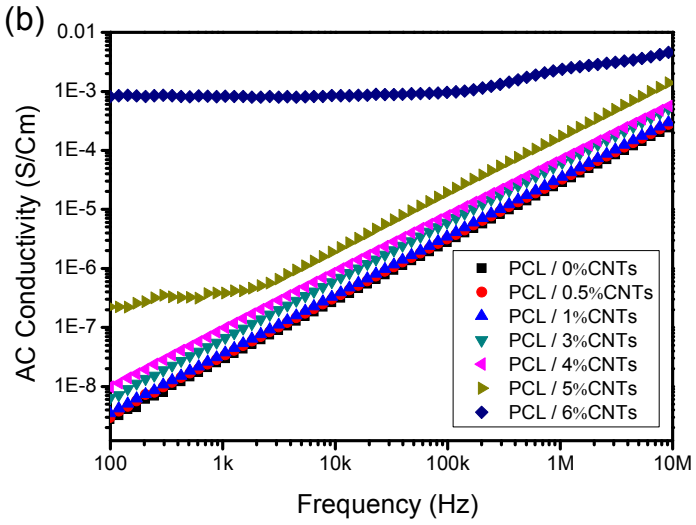

Figure 7. AC conductivity of the PCL ternary composites: (a) PCL/ImPCL/CNTs and (b) PCL/CNT series.

Electrical conductivity of the composites was determined by the concentration of conductive nanofillers in the matrix phase and structure continuity of the resulting composites [36]. The distribution of conductive nanofillers in the polymer blend and their interface characteristics are closely related to the electrical conductivity of the resulting composites. Figure 7 shows the AC conductivities of PCL/ImPCL/CNTs and PCL/CNTs composites with frequency ranging from 10^2 to 10^7 Hz at room temperature. The PCL blend and composites with 4 wt.% CNTs exhibit the typical frequency-dependent AC conductivity, which linearly increases with increasing frequency. However, composites with 5 wt.% CNTs exhibited AC conductivity independent of frequency change in the low frequency range. This result indicates the formation of effective three-dimensional conductive networks in the composites, so AC conductivity is independent of frequency change [37].

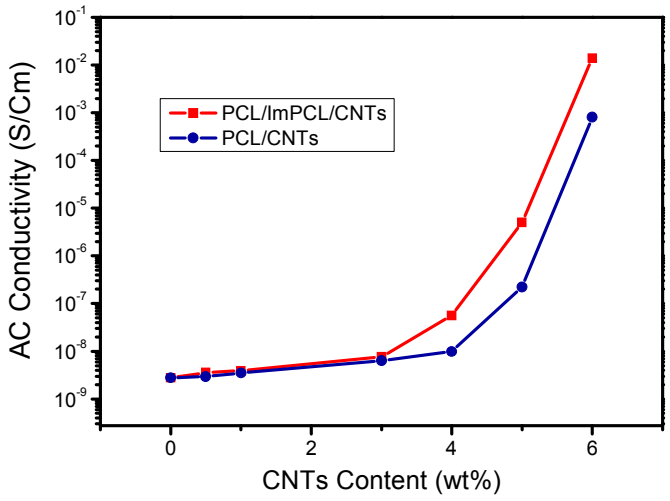

Figure 8. Changes in conductivity by increasing the CNT content of the composites with or without ImPCL.

The percolation threshold of conductive fillers was used to evaluate the electrical properties of the polymer composites. The electrical properties are considerably altered near the percolation threshold. Figure 8 shows the conductivity (σ) of the composites as a function of CNTs (wt.%) at 100 Hz. Conductivity does not significantly change at low contents (wt.%) of MWCNTs but increases by several orders of magnitude between 3–6 wt.% CNTs. The conductivity of PCL/CNTs without the block copolymer compatibilizer is lower than the corresponding PCL/ImPCL/CNTs because of the presence of aggregations. This indicates the higher amount of MWCNTs is required in PCL/CNTs to form effective three-dimensional conductive networks. The percolation effect is also directly related to the formation of three-dimensional conductive networks; consequently, improved nanofiller dispersion leads to a threshold recorded at low contents of CNTs [38-40]. The percolation threshold of the two series of composites was determined using the power laws, as follows:

$$\sigma_c \propto (fc - f)^{-t}, \text{ for } f \leq fc$$

where σ_c is the conductivity of the composites, f is the weight fraction of MWCNTs, fc is the critical weight fraction, and t is the critical exponent of conductivity that governs the scaling behavior in the region of fc. The optimal fitting of the experimental data to the power laws was achieved at fc = 3.1 wt.% for PCL/ImPCL/CNTs and fc = 4.9 wt.% for PCL/CNTs.

The obtained percolation threshold value of PCL/ImPCL/CNTs is lower than that of the

corresponding PCL/CNTs composite without compatibilizer. This decrease in the percolation threshold value of PCL/ImPCL/CNTs indicates that the compatibilizer plays dual roles: (a) avoiding reintegration of CNTs and (b) improving the affinity between the nanofillers and PCL matrix.

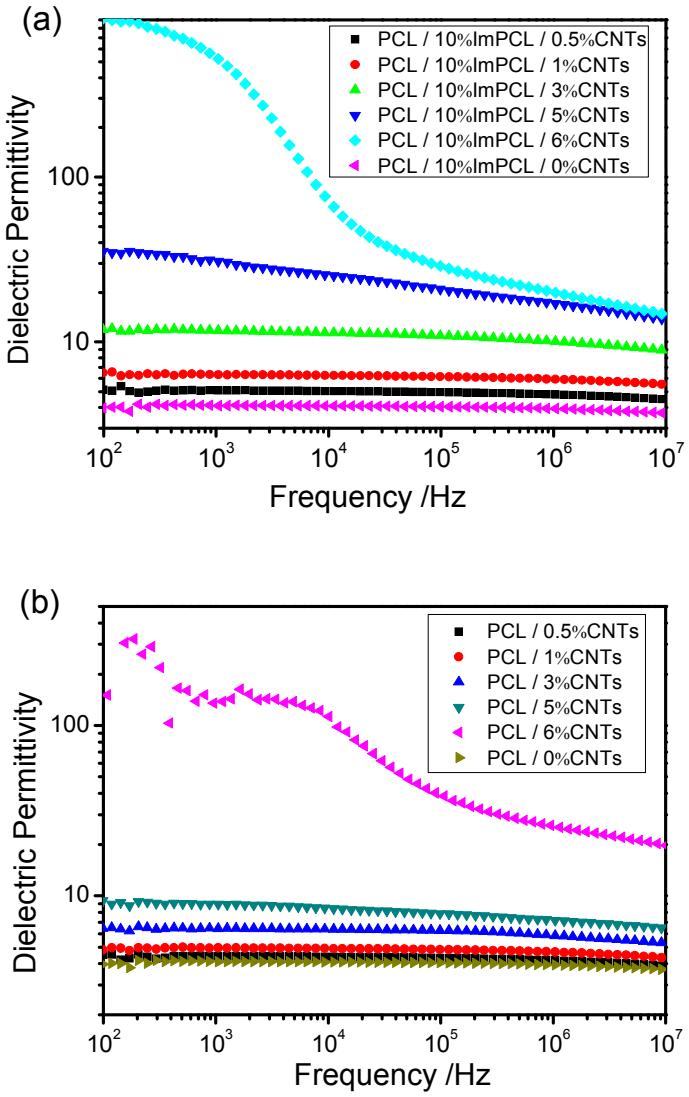

Figure 9. Dielectric properties of the PCL ternary composites: (a) PCL/ImPCL/CNTs and (b) PCL/CNTs series.

The permittivity of a material represents the ability to store charge when the material is subjected to an alternating electric field; as such, this parameter reflects the dielectric properties of the material. The composites containing conductive fillers generally exhibit a frequency-dependent permittivity, although the corresponding magnitudes vary. Studies showed

interfacial polarization, also known as the Maxwell–Wagner–Sillars effect, can induce a significant increase in permittivity at low frequency [41]. In our study, the dielectric permittivity of pure PCL sample at 1000 Hz was 4.09. The dielectric constant under the same frequency shows an increasing trend with increased CNTs contents (see in Figure 9 (B)). When at 6 wt.% CNTs, the dielectric constant of the material reaches 135.20 (1000 Hz), which is 30 times higher than that of PCL/0%CNTs. This characteristic is a typical dielectric property of conductive fillers/polymer composite system. The composites can be simulated by a large equivalent microcapacitor network between two testing electrodes, where the CNTs serve as microcapacitor electrodes and the polymer matrix serves as their dielectrics. As the CNTs loading increases, the mean distance between CNTs is dramatically reduced, thus leading to a high capacitance of the composites. Figure 9 (A) shows the permittivity of PCL/ImPCL/CNTs as a function of frequency range of 10^2–10^7 Hz at room temperature, and the tendency of variation was consistent with PCL/CNTs series.

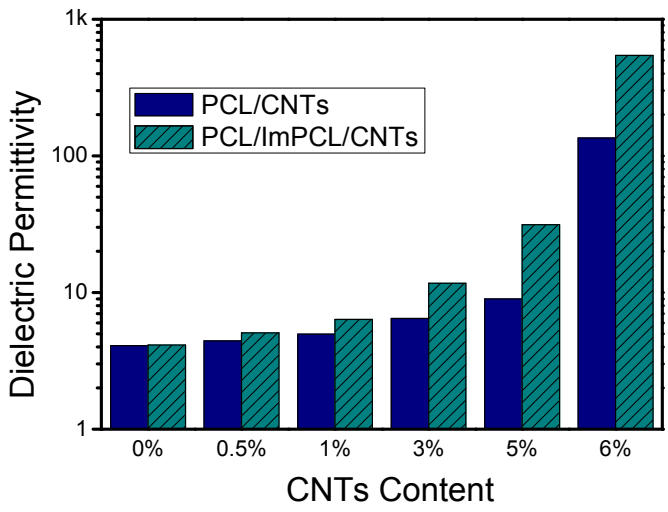

Figure 10. Dielectric permittivity of the PCL composites at 1000 Hz with and without ImPCL

As indicated in Figure 10, the dielectric permittivity of PCL/0.5%CNTs, PCL/1%CNTs, PCL/3%CNTs, PCL/5%CNTs and PCL/6%CNTs at 1000 Hz are 4.44, 4.97, 6.46, 8.97 and 135.20, while the parameter of PCL/ImPCL/CNTs with same CNTs loadings were 5.08, 6.34, 11.71, 31.35 and 544.16 respectively. The PCL/CNTs composites exhibit lower permittivity than the PCL/ImPCL/CNTs composites at the same CNTs content, which could be due to the formation of large agglomerates and entanglement in the polymer matrix. These agglomerates decrease the total

interface areas and increase the mean distance between CNTs in composites. While in the PCL/ImPCL/CNTs composites, the well dispersed conductive fillers are separated effectively by ImPCL and PCL matrix. As a result, more microcapacitors are formed and more free charges have been entrapped in the dielectrics between CNTs electrodes, so the dielectric constants of PCL/ImPCL/CNTs have greatly improved.

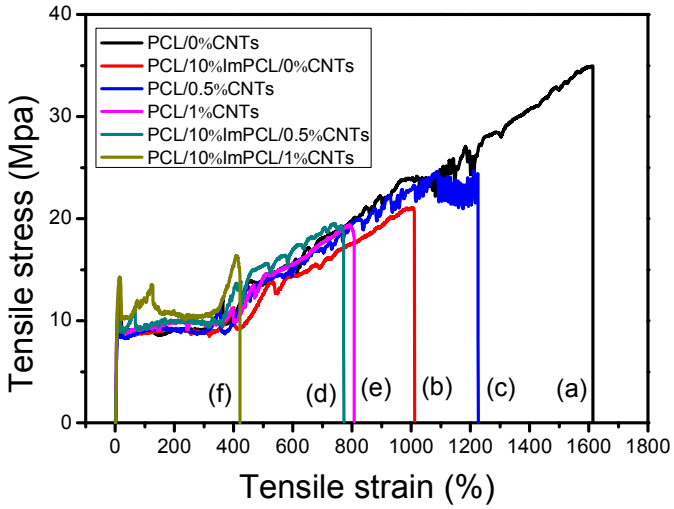

Figure 11. Stress–strain curves of PCL composites (a) PCL/0%CNTs, (b) PCL/10%ImPCL/0%CNTs, (c) PCL/0.5%CNTs, (d) PCL/10%ImPCL/0.5%CNTs, (e) PCL/1%CNTs and (f) PCL/10%ImPCL/1%CNTs.

Table 2. Mechanical properties of PCL composites

	Yielding strength (MPa)	Stress strength (MPa)	Elongation (%)	Young's modules (Mpa)
PCL/0%CNTs	12.60 (0.18)	31.58 (3.40)	1514.63 (98.80)	167.45 (14.69)
PCL/10%ImPCL/0%CNTs	12.38 (0.23)	21.79 (4.78)	1075.70 (125.21)	185.50 (16.84)
PCL/10%ImPCL/0.5%CNTs	12.82 (0.34)	19.45 (2.27)	803.38 (65.16)	197.68 (12.67)
PCL/10%ImPCL/1%CNTs	13.03 (0.31)	14.47 (1.91)	493.83 (83.30)	229.44 (16.08)
PCL/10%ImPCL/3%CNTs	13.12 (0.62)	13.12 (0.62)	12.90 (0.96)	249.85 (26.14)
PCL/10%ImPCL/5%CNTs	13.17 (0.38)	13.17 (0.38)	11.04 (1.68)	258.83 (13.69)
PCL/0.5%CNTs	12.05 (0.09)	23.29 (1.46)	1159.88 (52.76)	187.34 (16.18)
PCL/1%CNTs	12.03 (0.41)	17.93 (4.09)	705.24 (85.66)	198.15 (21.85)
PCL/3%CNTs	11.93 (0.24)	15.33 (1.48)	551.72 (100.44)	206.68 (33.50)

PCL/5%CNTs	11.49 (0.82)	11.72 (2.34)	313.42 (102.04)	215.86 (22.42)

The mechanical properties of the PCL composites were investigated with a tensile test. CNTs are commonly nanofiller which can reinforce the mechanical properties of polymer matrix when dispersed uniformly. As shown in Table 2, for all samples, Young's modules increases with the increasing of CNTs contents while elongation decreases. Owing to well dispersibility, PCL/ImPCL/CNTs samples show higher yielding strength and young's modules than PCL/CNTs samples. In addition, most specimens have a yielding point, followed by necking during the stretching, which is the typical tensile behavior for semi-crystalline PCL polymers. But when the CNTs content reached wt.3% in PCL/ImPCL/CNTs series, the elongation at break dramatic declined, so there was no remarkable necking or strain hardening process in sample PCL/10%ImPCL/3%CNTs and PCL/10%ImPCL/5%CNTs. The stress–strain curves for some typical samples with low CNTs loading, which showed high elongation and strain hardening, are depicted in Figure 11. Comparing PCL/10%ImPCL/0%CNTs and PCL/0%CNTs, we can observe that both the stress strength and elongation of PCL/10%ImPCL/0%CNTs are lower than PCL/0%CNTs because of the addition of low molecular weight PCL compatilizer. We can also find that the tensile stress of PCL/CNTs samples with different CNTs loadings (curve (a), (c) and (e)) at a same strain are very close to each other. This is because the poor dispersion and weak interfacial compatibility will weaken the effects of CNTs. On the contrary, the tensile stress of the PCL/ImPCL/CNTs samples at the same strain increase with the increased CNTs contents (curve (b), (d) and (f)), which is due to the improved compatibility with the help of ImPCL. Taken together, all these evidences confirm that the presence of ImPCL improved compatibility between CNTs and PCL matrix.

4. Conclusions

A synthesis strategy was developed by using ImPCL as compatibilizer to improve CNTs dispersion in the PCL matrix. The fabricated PCL/CNTs composites with ImPCL shows enhanced electronic and dielectric properties with a low percolation threshold (fc = 3.1 wt.%) than the composites without ImPCL. Compatibilizer coating on the surface of MWCNTs reinforces both CNTs dispersion and interface interaction between CNTs and PCL. Compared with typical acid

oxidation, modification does not cause structural damage to CNTs and exhibits strong practicability because commercial CNTs and PCL can be used directly without further treatment. This supramolecular strategy is a reliable and efficient pathway for CNTs dispersion while retaining intrinsic CNTs properties. Therefore, this physical modification of CNTs with ILs-based polymer can be used to prepare PCL composites with enhanced electrical properties for semi-industrial applications.

Acknowledgments

The authors gratefully acknowledge the National Natural Science Foundation of China for providing financial support (No. 51173009, 51573010).

References

1. S. Niyogi, M. Hamon, H. Hu, B. Zhao, P. Bhowmik, R. Sen, M. Itkis and R. Haddon, *Accounts of Chemical Research*, 2002, **35**, 1105-1113.
2. X. Peng and S. S. Wong, *Advanced Materials*, 2009, **21**, 625-642.
3. Z. Spitalsky, D. Tasis, K. Papagelis and C. Galiotis, *Progress in polymer science*, 2010, **35**, 357-401.
4. D. Sun, Z. Zhou, G.-X. Chen and Q. Li, *ACS Appl. Mater. Interfaces*, 2014, **6**, 18635-18643.
5. Q. Li, P. Peng, G. X. Chen and S. W. Yoon, *Journal of Materials Chemistry C*, 2014, **2**, 8216-8221.
6. Y. Xu, Q. Li, D. Sun, W. Zhang and G.-X. Chen, *Ind. Eng. Chem. Res.*, 2012, **51**, 13648-13654.
7. G.-X. Chen and H. Shimizu, *Polymer*, 2008, **49**, 943-951.
8. G.-X. Chen, H. Kim, B. Park and J. Yoon, *Polymer*, 2006, **47**, 4760-4767.
9. H. Kim, A. A. Abdala and C. W. Macosko, *Macromolecules*, 2010, **43**, 6515-6530.
10. D. W. Schaefer and R. S. Justice, *Macromolecules*, 2007, **40**, 8501-8517.
11. H. Bai, C. Li and G. Shi, *Advanced Materials*, 2011, **23**, 1089-1115.
12. M. Terrones, O. Martín, M. González, J. Pozuelo, B. Serrano, J. C. Cabanelas, S. M. Vega‐Díaz and J. Baselga, *Advanced Materials*, 2011, **23**, 5302-5310.
13. B. Zhao and W. J. Brittain, *Progress in Polymer Science*, 2000, **25**, 677-710.
14. J. Pyun, T. Kowalewski and K. Matyjaszewski, *Macromolecular Rapid Communications*, 2003, **24**, 1043-1059.
15. E. Manfredi, F. Meyer, P. Verge, J.-M. Raquez, J.-M. Thomassin, M. Alexandre, B. Dervaux, F. DuPrez, P. Van Der Voort and C. Jérôme, *Journal of Materials Chemistry*, 2011, **21**, 16190-16196.
16. K. Ul Hasan, M. O. Sandberg, O. Nur and M. Willander, *Nanoscale research letters*, 2011, **6**, 1-6.

17. X. Zhou, T. Wu, K. Ding, B. Hu, M. Hou and B. Han, *Chem. Commun.*, 2010, **46**, 386-388.
18. Q. Ji, I. Honma, S. M. Paek, M. Akada, J. P. Hill, A. Vinu and K. Ariga, *Angewandte Chemie*, 2010, **122**, 9931-9933.
19. S. Bellayer, J. W. Gilman, N. Eidelman, S. Bourbigot, X. Flambard, D. M. Fox, H. C. De Long and P. C. Trulove, *Advanced Functional Materials*, 2005, **15**, 910-916.
20. M. J. Park, J. K. Lee, B. S. Lee, Y.-W. Lee, I. S. Choi and S.-g. Lee, *Chemistry of materials*, 2006, **18**, 1546-1551.
21. S. Zhang, Y. Zhang, J. Zhang, Y. Chen, X. Li, J. Shi and Z. Guo, *Journal of materials science*, 2006, **41**, 3123-3126.
22. J. Wang, H. Chu and Y. Li, *ACS nano*, 2008, **2**, 2540-2546.
23. R. J. Chen, Y. Zhang, D. Wang and H. Dai, *Journal of the American Chemical Society*, 2001, **123**, 3838-3839.
24. Y.-L. Zhao and J. F. Stoddart, *Accounts of chemical research*, 2009, **42**, 1161-1171.
25. S. Bose, A. R. Bhattacharyya, A. R. Kulkarni and P. Pötschke, *Composites Science and Technology*, 2009, **69**, 365-372.
26. H. L. Zeng, C. Gao and D. Y. Yan, *Advanced Functional Materials*, 2006, **16**, 812-818.
27. S. J. Chin, S. Vempati, P. Dawson, M. Knite, A. Linarts, K. Ozols and T. McNally, *Polymer*, 2015, **58**, 209-221.
28. R. Bera, S. Maiti and B. B. Khatua, *Journal of Applied Polymer Science*, 2015, **132**.
29. T. Fukushima and T. Aida, *Chemistry-A European Journal*, 2007, **13**, 5048-5058.
30. F. Meyer, J.-M. Raquez, O. Coulembier, J. De Winter, P. Gerbaux and P. Dubois, *Chemical communications*, 2010, **46**, 5527-5529.
31. T. Biedroń, Ł. Pietrzak and P. Kubisa, *Journal of Polymer Science Part A: Polymer Chemistry*, 2011, **49**, 5239-5244.
32. Y. Ren, G.-X. Chen and Q. li, *Polymer Chemistry*, **submitted**.
33. R. Gao, M. Zhang, S. W. Wang, R. B. Moore, R. H. Colby and T. E. Long, *Macromolecular Chemistry and Physics*, 2013, **214**, 1027-1036.
34. A. Das, S. Pisana, B. Chakraborty, S. Piscanec, S. K. Saha, U. V. Waghmare, K. S. Novoselov, H. R. Krishnamurthy, A. K. Geim, A. C. Ferrari and A. K. Sood, *Nature Nanotechnology*, 2008, **3**, 210-215.
35. Z. Xu, Y. Niu, L. Yang, W. Xie, H. Li, Z. Gan and Z. Wang, *Polymer*, 2010, **51**, 730-737.
36. Z. Xu, Y. Zhang, Z. Wang, N. Sun and H. Li, *ACS applied materials & interfaces*, 2011, **3**, 4858-4864.
37. Y. Fu, L. Liu and J. Zhang, *ACS applied materials & interfaces*, 2014, **6**, 14069-14075.
38. F. Meyer, J.-M. Raquez, P. Verge, I. Martínez de Arenaza, B. Coto, P. Van Der Voort, E. Meaurio, B. Dervaux, J.-R. Sarasua and F. Du Prez, *Biomacromolecules*, 2011, **12**, 4086-4094.
39. C. W. Nan, Y. Shen and J. Ma, *Annu. Rev. Mater. Res.*, **2010**, **40**, 131-151.
40. C. W. Nan, *Prog. Mater. Sci.*, 1993, **37**, 1-116.
41. F. He, S. Lau, H. L. Chan and J. Fan, *Advanced Materials*, 2009, **21**, 710-715.

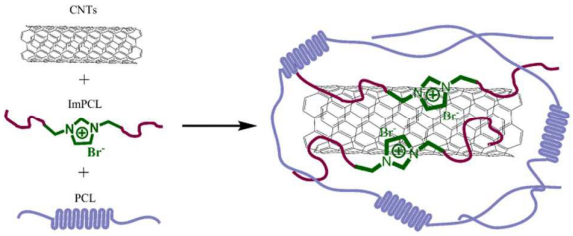

A compatilizer containing imidazolium segment was used to improve the compatibility of CNTs with PCL matrix.